E. M. Greitzer
Research Engineer,
Compressor Group,
Pratt & Whitney Aircraft,
East Hartford, Ct.

Surge and Rotating Stall in Axial Flow Compressors

Part II: Experimental Results and Comparison With Theory

This paper reports an experimental study of axial compressor surge and rotating stall. The experiments were carried out using a three stage axial flow compressor. With the experimental facility the physical parameters of the compression system could be independently varied so that their influence on the transient system behavior can be clearly seen. In addition, a new data analysis procedure has been developed, using a plenum mass balance, which enables the instantaneous compressor mass flow to be accurately calculated. This information is coupled to the unsteady pressure measurements to provide the first detailed quantitative picture of instantaneous compressor operation during both surge and rotating stall transients. The experimental results are compared to a theoretical model of the transient system response. The theoretical criterion for predicting which mode of compression system instability, rotating stall or surge, will occur is in good accord with the data. The basic scaling concepts that have been developed for relating transient data at different corrected speeds and geometrical parameters are also verified. Finally, the model is shown to provide an adequate quantitative description of the motion of the compression system operating point during the transients that occur subsequent to the onset of axial compressor stall.

Introduction

In a companion paper, presented as Part I,[1] several theoretical concepts were developed concerning the occurrence of rotating stall and surge in axial compressors. It was found that when uniform flow in an axial compressor becomes unstable, the mode of instability depends strongly on a nondimensional parameter, B, which can be defined in terms of the physical geometry of the system as

$$B = \frac{U}{2a}\left[V_p/(A_c L_c)\right]^{1/2}$$

Compression systems having a B above the critical value will exhibit the large amplitude mass flow and pressure oscillations that are associated with the term surge. For lower B the result of the instability will be operation in rotating stall at a substantially reduced flow and pressure rise.

This paper describes experiments that were carried out to quantitatively assess this theory, as well as to provide detailed information concerning transient compressor operation during rotating stall and surge.

Experimental Facility

The experimental program was carried out on a three stage axial compressor facility with a specially designed exit plenum chamber. The compressor had a constant area annulus with a 61.0 cm OD and a 0.7 hub/tip ratio. The blading consisted of three repeating stages, using NACA 400 series airfoils, plus inlet and exit guide vane rows. In order to withstand the prolonged running in rotating stall and surge, the blading was machined from stainless steel, except for the exit guide vane, which was aluminum.

The compressor is driven by an electric motor and the speed can be continuously varied up to the maximum value used. The highest corrected speed used in the present set of experiments was 3420 rpm, corresponding to a rotor velocity at midspan of 92.9 m/s.

The dimensions of the plenum were chosen based on a design study using the theory developed in Part I. The plenum was sized

[1] Greitzer, E. M., "Surge and Rotating Stall in Axial Flow Compressors—Part I: Theoretical Compression System Model."

Contributed by the Gas Turbine Division and presented at the Gas Turbine Conference, Houston, Texas, March 2–6, 1975, of THE AMERICAN SOCIETY OF MECHANICAL ENGINEERS. Manuscript received at ASME Headquarters November 22, 1974. Paper No. 75-GT-10.

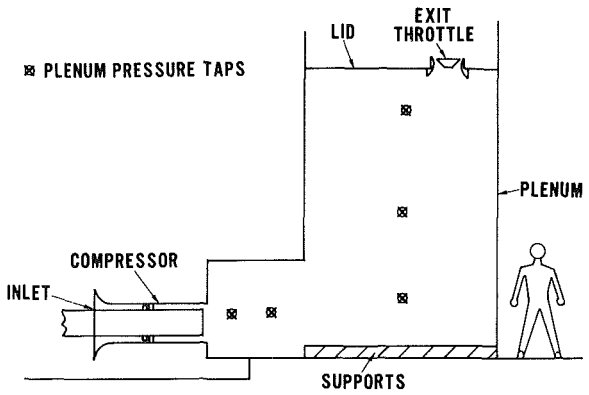

Fig. 1 Scale section of compressor/plenum configuration

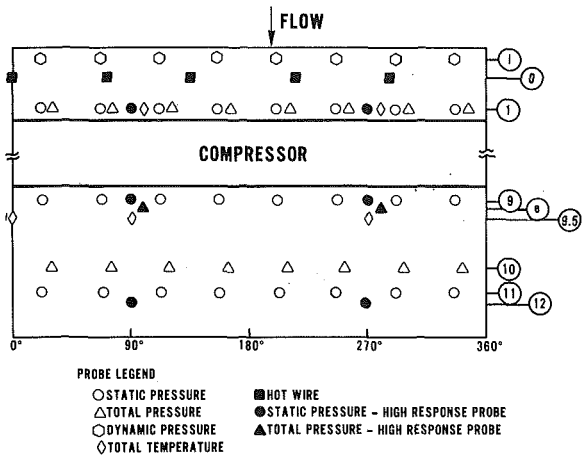

Fig. 2 Instrumentation locations in compressor

so that surge could be achieved over a substantial speed range using the present compressor. However, it should be noted that according to the theory, the use of higher wheel speed and a greater number of stages (such as is the case in a conventional multistage compressor) will tend to markedly reduce the plenum volume needed to obtain surge.

A schematic of the facility, which is approximately to scale, is shown as Fig. 1. The air was drawn into the compressor from a large room at essentially atmospheric conditions. After leaving the compressor the flowpath consisted of a 0.46 m long exit duct having the same inner and outer diameters as the compressor annulus. This duct discharged into a large plenum, with the flow rate being controlled by a throttle on the downstream side of this plenum. The throttle was an annular passage whose area could be controlled by translating a center cone. Two types of exit plenum were used. The first was a 1.53 m dia pipe, 1.5 m in length. In the second configuration, which is the one illustrated in Fig. 1, this pipe was used as a transition between the compressor exit duct and a 3.05 m dia, 5.2 m high vertical cylindrical chamber. This latter plenum had a lid in it which contained the exit throttle, and the height of this lid could be varied to change the total plenum volume. The lid, as well as the floor of the chamber, was gusseted, so that the volume of the plenum would remain constant in spite of the large amplitude loads that were expected. Four different volumes were tested corresponding to having the lid at three different heights, as well as using the 1.53 m dia pipe by itself with a plate containing the throttle welded on the end. The plenum volumes corresponding to these different configurations were 34.9, 22.8, 15.0, and 2.8 m^3.

Both steady-state and high response instrumentation were used. The steady-state instrumentation was used to define the compressor performance curve which is needed for the calculation procedure discussed in Part I.

The location of the instrumentation is shown in Figs. 1 and 2. Fig. 1 gives the location of the plenum pressure taps, with each position having provision for both a high response transducer and a steady-state measurement line. The probes that were installed in the compressor duct are presented in Fig. 2 which is an "unrolled" view of the compressor annulus. Additional instrumentation, such as stator mounted hot films, was also utilized for more detailed flow field diagnosis.

The steady state data was recorded using the United Aircraft Research Laboratories computerized data system. Hot wires and high response pressure transducers were used to obtain information about the time varying flow occurring during rotating stall and surge. The transducers used were bonded strain gauge MB/Alinco differential types. The data were recorded on magnetic tapes as an analog signal then later converted to digitized form for quantitative data reduction purposes.

Compressor Characteristic-Steady-State Data

For the present purposes, the most relevant compressor characteristic is the nondimensionalized curve of plenum pressure minus atmospheric pressure, $\Delta P/(\frac{1}{2}\rho U^2)$, versus inlet C_x/U. It is emphasized that the value of C_x that is used is an annulus averaged value. In situations where the compressor was not operating in ro-

Nomenclature

a = speed of sound
A = flow-through area
B = dimensionless number, defined in equation (14)
C_P = specific heat
C_V = specific heat
C_x = axial velocity
h_0 = stagnation enthalpy per unit mass
i = incidence angle on blade trailing edge
k = polytropic exponent
L = effective length
m = mass flow
$N/\sqrt{\theta}$ = corrected rotor rotational speed (rpm)
P = pressure
ΔP = plenum pressure rise, $(P_{\text{plenum}} - P_{\text{ambient}})$
$\dot{Q}$ = rate of heat transfer to plenum
t = time
T = temperature
T_0 = stagnation temperature
U = mean rotor velocity
V_p = plenum volume
x = axial distance
γ = specific heat ratio
δ = variation in plenum thermodynamic quantities during a surge cycle
ϵ = error in calculated compressor mass flow due to isentropic assumption, see equation (A-4)
ρ = density
ω = helmholtz resonator frequency: $\omega = a\sqrt{\frac{A_c}{V_p L_c}}$

Subscripts

1 = compressor discharge (plenum inlet)
2 = plenum exit
c = compressor
T = throttle exit
isen = calculated using an isentropic P-ρ relationship for the plenum
p = plenum
min = minimum value during a surge cycle
max = maximum value during a surge cycle

Superscripts

$-$ = time mean

tating stall this could be measured by standard inlet instrumentation, which is placed several chords upstream of the inlet guide vanes. However, for the rotating stall regime, the strongly asymmetric, unsteady flow field which is associated with the blockage of the stall cell can lead to substantial errors in this measurement if a conventional instrumentation set up is used. Therefore, the far downstream exit throttle was calibrated and used to measure mass flow in this regime.

The compressor characteristic for one corrected speed is shown in Fig. 3. The hysteresis behavior obtained for the initiation and cessation of rotating stall, which has been mentioned by other investigators, is evident. There are slight differences in the curves of the different corrected speeds due to compressibility and increased Reynolds numbers at the higher speeds. However, since the maximum pressure ratio is 1.07, and the minimum Reynolds number is well over 10^5 even for the lowest speed used, these effects are quite small. This steady-state data was taken at mean wheel speeds of 30.5, 43.9, 59.0, 76.2, and 92.9 m/s.

The data presented in Fig. 3 was obtained with two different plenum volumes. It can be seen that there is minimal effect of volume on the compressor characteristic for a given corrected speed. In particular, the nondimensional axial velocity parameter at which the compressor encountered stall, i.e., the uniform flow stability limit, was found to be constant within experimental accuracy over the range of volumes tested in the present series of experiments.

Data Analysis—Unsteady Flow Measurements

As mentioned, it is desired to obtain the transient operating points through which the compression system moves during the cyclic behavior that characterizes surge, as well as during the departure from one equilibrium point and approach to another (at a reduced flow and pressure rise) that is associated with stable operation in rotating stall. This task is complicated by the fact that during part or all of these transients the compressor is operating with rotating stall present. Thus not only is the annulus averaged flow time varying, but the flow is also severely nonuniform around the circumference. This is an important aspect of the flow measurement process. It implies that the instantaneous compressor mass flow cannot be measured with the desired precision by probes (e.g., hot wires) which are either within the upstream potential field of the rotating stall cell or are downstream of the compressor, unless one has a reasonably large number of sensors that are distributed over the annulus to give an instantaneous annulus averaged flow as a function of time. (An alternative procedure would be to place a probe far enough upstream of the compressor so that it would be out of the potential field of the stall cell and the flow in the annulus would be axisymmetric. This means an upstream distance on the order of half a circumference, and was undesirable in the present experiment for two reasons. First it would decrease the maximum value of B that could be obtained in the experiment, since the effective length of the compressor passage would be increased; and second, it was not very feasible with the compressor drive configuration that was available.)

To avoid this problem, a new procedure was developed for calculating the compressor mass flow, using the calibrated throttle and a continuity balance in the plenum. This procedure is based on the fact that the mass flow through the compressor is equal to the sum of the rate of increase of mass in the plenum and the mass flow through the throttle. Hence, if these two quantities can be calculated, we can readily obtain the instantaneous annulus averaged compressor mass flow.[2]

In order to carry out this calculation, it is necessary to know the instantaneous state of the fluid in the plenum. To obtain this information, a substantial effort was put into a data reduction procedure for the unsteady plenum pressure measurements that were the primary input. The data was first recorded on magnetic tape as an analog signal, with selected sections digitized in five second segments. The digital data was then run through a calibration conversion, with the resulting output used as input to the program that calculated the time dependent thermodynamic and flow quantities. This final program read the digital data (the unsteady pressures in the plenum) at 208 interals per s, smoothed it, and locally fitted cubic spline curves through all the points.

These operations were necessary because derivatives of the primary data were required. Careful checking of both the pressure output from the program and its derivative with different amounts of smoothing, as well as comparison of fits using curves of different orders was done before the final form of the procedure was decided upon, in order to ensure that no spurious results would be introduced by the numerical operations. Once having the plenum pressure and its derivative at the approximately 10^3 points in each five second segment (5×208), the instantaneous annulus-averaged inlet mass flow and axial velocity parameter, as well as the nondimensional plenum pressure, could be calculated and output at a specified time interval using the methods discussed in the following.

It should be noted that this procedure was not restricted to using data from a single channel. There were usually from four to six transducers in the plenum whose outputs were recorded and put through the procedure, and the calculation could be made using averages of the pressures recorded by any two channels. However, it was found that the averaging yielded results that were virtually identical to those of a single channel, and for convenience some of the later data reduction was carried out on this basis, with frequent checks to ensure that this was still the case.

The analytical approach to calculating the flow quantities can be discussed in two phases, the calculation of the throttle exit mass flow, and the calculation of the rate of increase of mass in the plenum.

Let us consider the flow through the throttle. The ratio $[(P_{\text{plenum}} - P_{\text{atmospheric}})/P_{\text{atmospheric}}]$ is quite low for the situations encountered in the present experiment (the maximum value is less than 0.09). In addition, the frequencies that characterize the unsteady compression system behavior are also very low. Because of this, an accurate approximate method for calculating the throttle flow can be developed based on an iterative procedure. In the situation examined, it is a good approximation to regard the fluid velocity at the exit throttle as depending on the instantaneous plenum pressure and density as if the flow were incompressible and steady. This "zeroth order" approximation for the instantaneous velocity at the exit throat can be written:

$$C_{x_T} = \left[2\,\frac{(P_{\text{plenum}} - P_{\text{atmospheric}})}{\rho_{\text{plenum}}}\right]^{1/2} \tag{1}$$

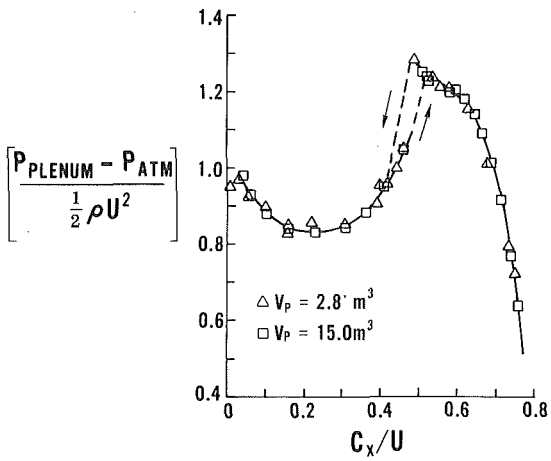

Fig. 3 Steady-state compressor characteristic

[2] The initial suggestion concerning the possibility of this approach was made by the late Prof. A. H. Stenning.

However, the actual flow is (slightly) unsteady and compressible. Therefore, to find an improved value for the throat velocity, we use the one-dimensional unsteady compressible flow equations, and work to one order higher in the quantity M_T^2 than in the above expression and to first order in powers of a frequency parameter characterizing the oscillations. Consistent with retaining terms of this order, we can use our zeroth order velocity in approximating the small correction terms. Thus a term like $(1 + M_T^2/4)^{1/2}$, which includes the small correction for compressibility can be expressed to this order as:

$$[1 + M_T^2/4]^{1/2} = [1 + \rho_T C_{x_T}^2/(4\gamma P_T)]^{1/2} \cong [1 + \Delta P/(4\gamma P_T)] \quad (2)$$

Since the maximum value of the correction term was less than 0.02, the use of the approximation is amply justified.

The correction for unsteadiness is handled in an analogous fashion, utilizing the zeroth order solution to give a very good approximation to the small correction which arises from the fact that, in an unsteady one-dimensional flow, the stagnation temperature can vary along a streamline even if the flow is isentropic,[3] i.e.,

$$\frac{\partial h_0}{\partial x} = -\frac{\partial C_x}{\partial t} \quad (3)$$

and this change in total temperature makes the stagnation conditions at the throat *slightly* different from those in the plenum.

These two corrections are quite small, with their combined magnitude not exceeding approximately three percent of the initial, zeroth order value for throttle velocity, so that only one iteration was used. An explicit expression can thus be written for C_{x_T} in terms of the pressures and density:

$$C_{x_T} = [\frac{2\Delta P}{\rho_p}]^{1/2}[1 + \frac{\Delta P}{4\gamma P_T}] - \frac{L_T}{2}\frac{1}{\Delta P}\frac{d}{dt}\Delta P \quad (4)$$

The instantaneous exit velocity can then be used with the instantaneous value of the density at the exit and the known throttle exit area to find the mass flow through the throttle, $\dot{m}_T$, as a function of time:

$$\dot{m}_T(t) = A_T \rho_T(t) C_{x_T}(t) \quad (5)$$

Since there is negligible mass storage in the short throttle passage, the plenum exit mass flow can be taken equal to the throttle exit mass flow

$$\dot{m}_2 = \dot{m}_T \quad (6)$$

However we still cannot solve for $\dot{m}_2$ unless we are able to calculate the density at the throttle and in the plenum, and this can only be done if the thermodynamic state of the fluid in the plenum is known. Therefore let us now consider the conditions in the plenum.

The continuity equation for the plenum can be written (see Fig. 4) as:

$$\dot{m}_1 = \dot{m}_2 + V_p \frac{d\rho_p}{dt} \quad (7)$$

where the density is taken to be the instantaneous average value throughout the plenum. Using the equation of state, and the assumption of negligible velocity in the plenum this can be written as:

$$\dot{m}_1 = \dot{m}_2 + \rho_p V_p (\frac{1}{P_p}\frac{dP_p}{dt} - \frac{1}{T_p}\frac{dT_p}{dt}) \quad (8)$$

The First Law applied to the plenum is:

$$\dot{m}_1 C_P T_{0_1} = \dot{m}_2 C_P T_{0_2} + V_p \frac{d}{dt}(\rho_p C_V T_p) + \dot{Q} \quad (9)$$

Since heat transfer calculations show that there is no significant heat transfer from the plenum, the plenum flow can be considered adiabatic and $\dot{Q}$ can be neglected. In addition, the stagnation temperature of the flow leaving the plenum is equal to the temperature of the gas in the plenum, so that equation (9) can be expressed as:

$$\dot{m}_1(\frac{T_{0_1}}{T_p}) = \dot{m}_2 + \frac{\rho_p V_p}{\gamma P_p}\frac{dP_p}{dt}. \quad (10)$$

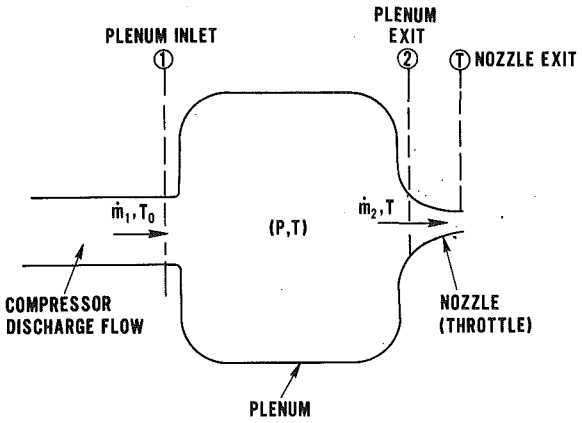

Fig. 4 Control volume for data analysis

In order to obtain the exit mass flow through the compressor, two alternative approaches were used. The first was a numerical integration of the coupled nonlinear equations for C_{x_T}, T_p, $\dot{m}_1$, $\dot{m}_2$, and $\dot{m}_T$, equations (4), (5), (6), (8), and (10), using the measured unsteady pressures as input. In this procedure the quasi-steady measured compressor temperature rise curve was input to provide the value of the stagnation temperature of the entering flow as a (nonlinear) function of the compressor mass flow. Since the values of the plenum flow quantities were only weakly dependent on the exact shape of this curve, due to the fact that the overall compressor temperature ratio is close to unity, the departure from quasi-steady compressor behavior that actually occurs has only a small effect on the final results. Once the exit mass flow was known, the inlet axial velocity could then be calculated and normalized by mean rotor speed to give the nondimensional axial velocity parameter, C_x/U.

In order to lessen the amount of computing time involved in putting a large amount of data (only a small part of which is shown in this paper) through the numerical integration scheme, a second procedure was also developed. This latter procedure, although substantially shorter, gave virtually the same result as the former one, the two being within one percent of each other for all cases in which the two were compared. All of the digitized data were reduced using the shorter method, while roughly one-third was also reduced using the more lengthy procedure so that this comparison was made over the whole representative range of flow conditions that were investigated.

The principle behind the second procedure was based on the fact that the ratio of compressor discharge stagnation temperature and plenum temperature is very close to unity (it differs by approximately two percent or less for almost all flow conditions during which significant mass flow enters the plenum) because of the low overall temperature rise of the compressor. Therefore, the changes in plenum density or temperature that are associated with a given change in plenum pressure are extremely close to those which occur during an isentropic expansion or compression of the fluid *in the plenum.*

Hence, if one were trying to compute the time variations of the thermodynamic state of the fluid in the plenum using the pressure variations as a known quantity, it would be anticipated that an excellent approximation would be to assume that: (1) the temperature change is the same as that which occurs in a process with no

[3] Dean, R. C., "On the Necessity of Unsteady Flow in Fluid Machines," ASME *Journal of Basic Engineering*, Vol. 81, Mar. 1959, pp. 24–29

entropy change, and (2) more importantly, that the use of this approximation would lead to very small errors in the final calculation for $\dot{m}_1$, which is the quantity of interest.

A plausibility argument for this procedure can be generated by rewriting equation (10) as:

$$\dot{m}_1 = \frac{\dot{m}_2 + \frac{\rho_p V_p}{\gamma P_p}\frac{dP_p}{dt}}{1 + (T_{0_1} - T_p)/T_p} \tag{11}$$

It is seen that if the term $[(T_{0_1} - T_p)/T_p]$ has an amplitude of 0.02, say, as mentioned before, a quite accurate approximation for $\dot{m}_1$ would be given by simply neglecting this term and using the isentropic P-ρ relationship. A fuller examination of this argument, which is presented in the Appendix, shows that this is indeed the case, as does the close agreement of the results to those obtained by integrating the coupled differential equations.

If this approximation is made, the equations to be solved become algebraic relations between the unsteady pressure measurements, which are the input data, and the throttle and compressor mass flows. Making use of equation (6), these are:

$$\dot{m}_T = \rho_T C_{x_T} A_T \tag{12}$$

and

$$\dot{m}_1 = \dot{m}_T + \frac{\rho_p V_p}{\gamma P_p}\frac{dP_p}{dt} \tag{13}$$

The velocity at the throttle, C_{x_T}, is given by equation (4), ρ_T is again calculated using the one-dimensional unsteady flow equations and the instantaneous plenum conditions, and changes in ρ_p and P_p are related by isentropic relations.

Even when using this simplified procedure, however, some iteration was done, in that the calculation was first carried out with the time mean plenum temperature given by the steady-state value corresponding to a given throttle setting, and the result of this used to define a corrected version of the curve of time mean temperature versus throttle setting, which was then used in the second run of the calculation.

Overall Compression System Behavior in Rotating Stall and Surge

Rotating Stall. The hot wires and high response pressure probes showed that the rotating stall pattern observed with this compressor was a single cell rotating at between twenty-five and thirty percent of the rotor speed, with the exact speed depending slightly on corrected speed and compressor operating point. It was found that the magnitudes of the static pressure fluctuations at the exit of the compressor were approximately sixty percent of those at the inlet, i.e., the latter were not negligible compared to the former, as has sometimes been assumed in analytical treatments of rotating stall in axial compressors. However, pressure measurements in the *plenum* during rotating stall showed negligible static pressure variation with time. Therefore, during rotating stall, even though the flow in the *compressor* is nonsteady as well as spatially nonuniform, the *compression system* behavior, as represented by the plenum pressure and annulus averaged mass flow, is quite steady and the range of operation from shutoff to where the compressor characteristic curve rises sharply can be considered a stable one.

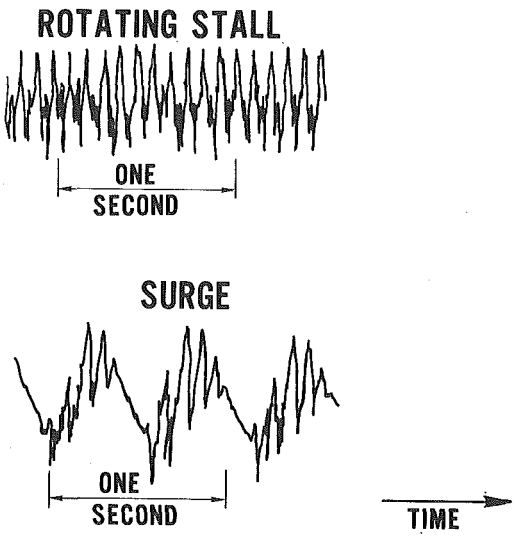

Fig. 5 Hot wire output at compressor inlet

Surge. The pure rotating stall was found during operation with the small volume and at low speed with the large volumes—in other words for low values of the parameter, B. At higher values of B, as indicated by the numerical results of Part I, the *system* did not show a steady behavior, but exhibited the large amplitude oscillations associated with surge.

The qualitative difference between the two types of behavior is presented in Fig. 5, which shows a tracing of an oscillograph record of the output of a hot wire at the rotor inlet. The data shown were taken at the same corrected speed but with different plenum volumes. During the surge cycles that are shown, the compressor can be seen to pass in and out of rotating stall, with the rotating stall characteristics appearing to be quite similar to those obtained during steady-state operation. In particular one can see that the frequency with which the stall cells pass the hot wire is essentially the same in the two cases.

Inception of Surge—Comparison with Theory

The most basic prediction of the theory that has been developed is that, for a given compressor characteristic and throttle geometry, the point at which the mode of compressor instability changes from rotating stall to surge is dependent upon the parameter, B, which can be written in terms of the physical parameters of the experiment as:

$$B = \frac{U}{2\omega L_c} \tag{14a}$$

$$= \frac{U}{2a}\left[V_p/(A_c L_c)\right]^{1/2} \tag{14b}$$

To test this, the compressor was run past the uniform flow stability limit (stall limit line) at different speeds with each of the four volumes, in order to find the lowest corrected speed at which a surge oscillation would occur for each of the volumes. It was found that the boundary between the occurrence of rotating stall and surge was relatively sharp, the change taking place over a difference in corrected speeds of roughly 100 rpm (a change of less than 5 percent in corrected speed). At the lower end of this range the compressor would exhibit almost constant amplitude rotating stall, similar to that shown in Fig. 5, when the stall line was crossed. On a speed line at a slightly higher corrected speed, the amplitude of the rotating stall cells would have strong modulations at the surge frequency. Increasing the speed still further would lead to the occurrence of a surge oscillation, where over a portion of the cycle the compressor would be instantaneously operating free from rotating stall, even though the throttle setting was below the uniform flow stability limit.

The conditions at which the mode of instability changes from rotating stall to surge are plotted in Fig. 6. This shows the parameter B, which should be constant (if the nondimensional compressor curves were exactly the same at all speeds), plotted against corrected speeds, with the regions in which surge or rotating stall would be encountered also shown. It can be seen that the prediction of constant B is quite well borne out, although the absolute value of this parameter at which the change occurs is somewhat above that predicted by the theory.

Transient Compression System Behavior

Using the data reduction program described above, the transient compression system behavior can be displayed in a manner similar to that used in Part I. This is done in Figs. 7–12. The nondimen-

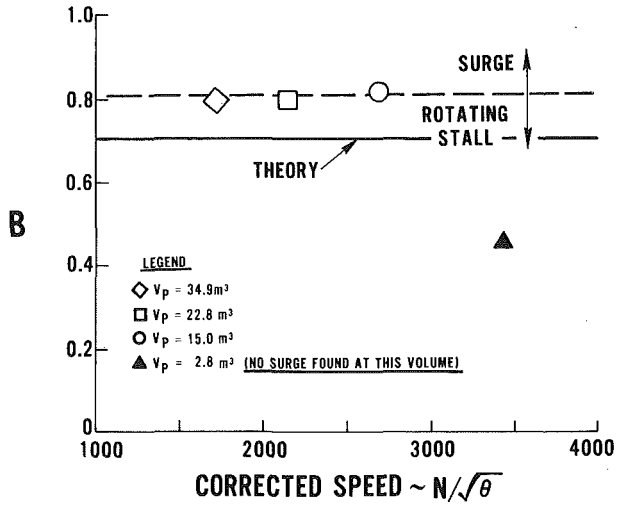

Fig. 6 Onset of surge for different plenum volumes

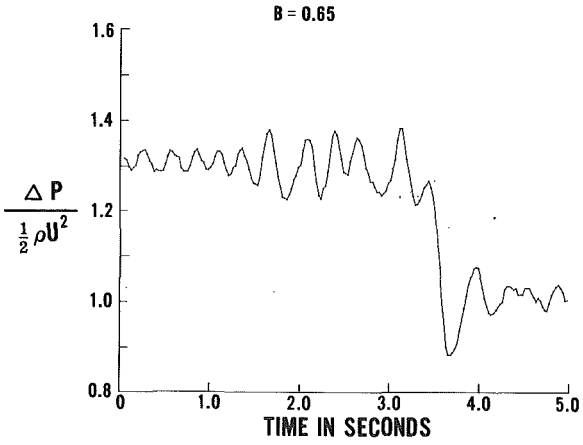

Fig. 7(a) Transient compression system response: B = 0.65

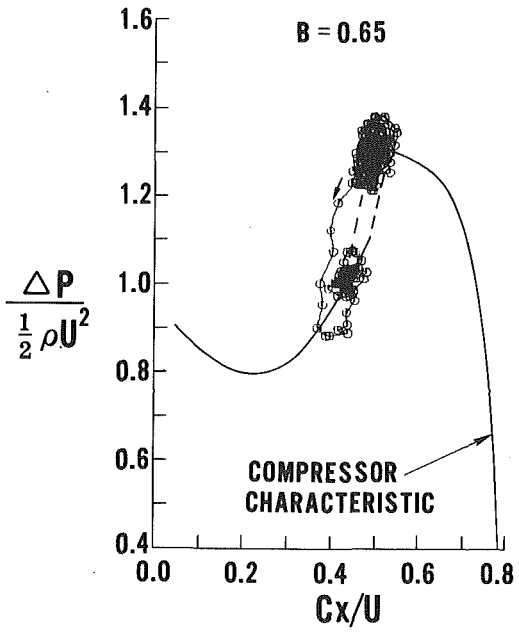

Fig. 7(b) Transient compression system response: B = 0.65

sional plenum pressure rise, $\Delta P/\frac{1}{2}\rho U^2$, and the axial velocity parameter, C_x/U, are presented versus time, as well as being plotted against each other in a compressor performance map type of representation. In this latter type of plot, the measured steady state characteristic is shown for reference. Each symbol that appears in the figures (each dot in the plots of parameters versus time, each open box in the plots of $\Delta P/\frac{1}{2}\rho U^2$ versus C_x/U) represents a calculation of plenum pressure rise and axial velocity parameter. To obtain good resolution of the motion, the interval at which the calculations were done was kept short enough so that at least twenty, and usually approximately thirty, points were calculated during each cycle. The actual time intervals that were used ranged from 0.025 s to 0.015 s, which was used for the higher frequency surges.

The estimated uncertainty in the data is approximately ±2 percent for the transient pressures and ±5 percent for the transient axial velocity parameter for the higher speed runs, with slightly higher values for the lower speed data. It should be emphasized that these errors are quite small compared to the variation in the quantities themselves, and the data can be considered to give a very good representation of the transient motion of the system operating point. Verification as to the consistency of the data can be seen in the agreement between the initial operating point given by the transient data and the steady-state compressor stall point.

We first examine the stall transients occurring along a constant compressor speed line as a function of B. This is the response that is encountered when the compressor is initially operating with uniform flow and the throttle is then closed enough so that the compressor operating point is moved past the point of instability for uniform flow (stall limit line). Figs. 7*(a)* and 7*(b)* show the system transient that occurred with a corrected speed of 59.0 m/s, a plenum volume of 15.0 m^3, and an effective compressor length, L_c, of 1.8 m, corresponding to a value of B = 0.65. This value of L_c will be maintained in all the experiments discussed below, unless specifically mentioned.

The theoretical prediction, based on the model of Part I, is that at this value of B the compression system should become unstable at the stall line, and should then move to a new stable operating point at a considerably lower pressure rise and flow rate. This behavior can be seen in Figs. 7*(a)* and 7*(b)*. After becoming unstable at the initial operating point, the system undergoes a large amplitude transient to another operating point at which it exhibits the damped oscillatory behavior that is characteristic of stable equilibrium. Although it is not shown because of the five second limit of the digitizing, the analog records indicate that the oscillation amplitude does decrease further with time, to a level that is low enough such that the mass flow and plenum pressure can be regarded as steady-state. Note that at this new equilibrium point the compressor is in rotating stall.

Figs. 8*(a)*, 8*(b)*, and 8*(c)* show the system behavior at the same corrected compressor speed, but with an exit plenum volume of 34.9 m^3, so that the value of B is 1.00. The analysis indicates that at this value there will not be a stable operating point past the stall line, and the system will exhibit the limit cycle type of oscillation that characterizes surge. The data in Figs. 8*(a)* and 8*(b)* show that the system is now more strongly unstable as the stall line is reached, and the transient from this point occurs somewhat more abruptly, leading now to a surge cycle oscillation rather than rotating stall. During the surge cycle the inlet hot wires show that the compressor passes in and out of rotating stall as the mass flow changes, in a manner similar to that shown in Fig. 5.

A basic conclusion of the theory that has been developed is that, at the same value of B, the compression system will exhibit the same transient behavior, independent of whether this value is obtained with a large volume and a low speed or a small volume and a high speed (neglecting the minor differences in the compressor characteristic).[4] Fig. 9 shows data taken at a corrected speed of 92.9 m/s and a plenum volume of 15.0 m^3, which corresponds to a value of B of 1.03. This can be directly compared to Fig. 8*(c)*,

[4] When represented as a plot of the nondimensionalized variables C_x/U versus $\Delta P/\frac{1}{2}\rho U^2$.

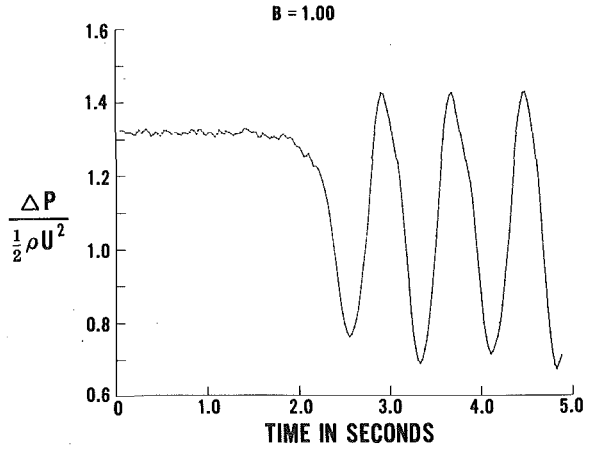

Fig. 8*(a)* Transient compression system response: $B = 1.00$

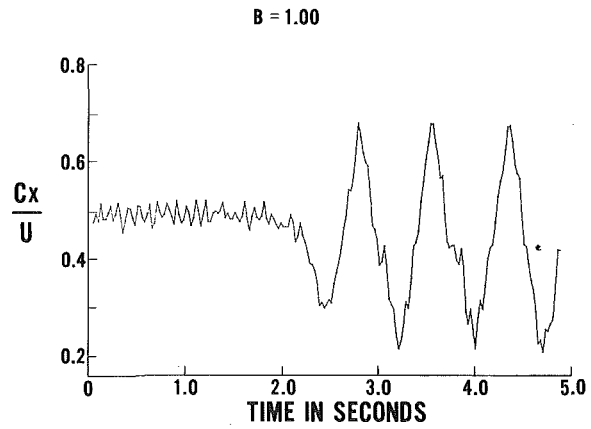

Fig. 8*(b)* Transient compression system response: $B = 1.00$

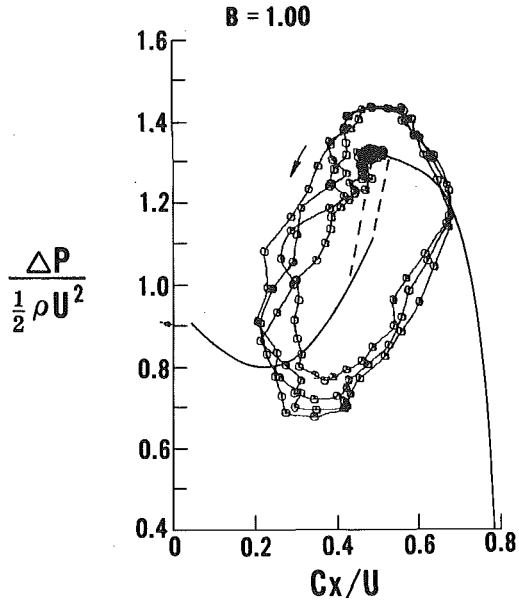

Fig. 8*(c)* Transient compression system response: (low speed, large volume): $B = 1.00$

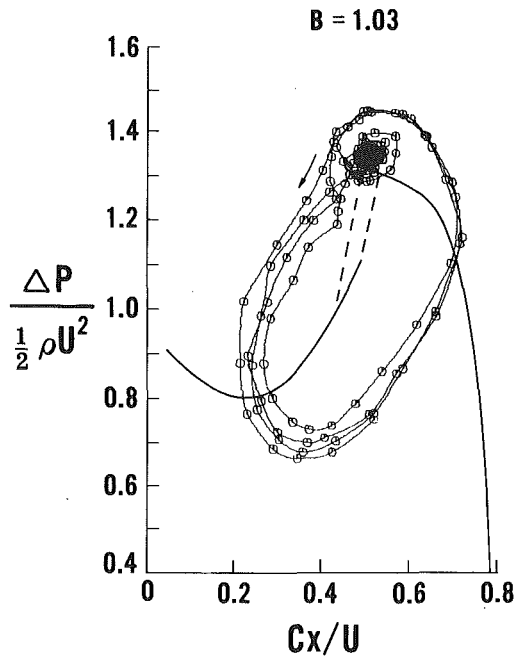

Fig. 9 Transient compression system response: (high speed, small volume): $B = 1.03$

which is at essentially the same value. The two surge cycles show extremely similar behavior, emphasizing the influence of B as the relevant nondimensional parameter for the phenomenon under study.

It has been shown that, as B is increased, the post stall behavior of the compression system can change from rotating stall to surge. As pointed out in Part I, there is also a strong influence of this parameter on the character of the surge oscillations that occur. This can be seen in Figs. 10, 11, and 12, which complement Figs. 7*(b)*, and 8*(c)*/9, to show the system behavior over a range of values of B. Fig. 10 is for a B of 0.84, which is only slightly above the critical B needed for surge to occur. Fig. 11 is for $B = 1.29$, and Fig. 12 is for $B = 1.58$, the largest value that was obtained. For clarity, the theoretical curves are only indicated in the figures for one representative case, $B = 1.29$ (this was actually a truly representative case, the agreement being slightly better at the higher values of B and slightly worse at the lower). However, an additional comparison can be made with the theoretical results for $B = 1.58$ which have appeared as Fig. 7*(b)* in Part I. It can be seen that the overall agreement is quite reasonable, with the major discrepancy occurring near zero flow where the transient compressor behavior is not at all well understood.

As B is increased the oscillations can be seen to assume a more circular path when plotted in the compressor map format, with the excursions in mass flow becoming significantly larger, and those in plenum pressure rise remaining relatively constant or even decreasing slightly. This same trend is also clearly indicated in the analytical results of Part I, which cover roughly the same range (compare the curves in Figs. 6*(b)* and 7*(b)* in Part I).

A physical argument can be given for this change in the shape of the limit cycle curves as B is increased. Notice that B can be written as:

$$B = \frac{\frac{1}{2}\rho U^2 A_c}{\rho \omega U L_c A_c}$$

For a given compressor, the numerator, which is proportional to the magnitude of the pressure differential across the compressor duct ($P_{\text{plenum}} - P_{\text{atmospheric}}$), represents the driving force for the acceleration of the fluid in the duct. If we consider oscillations that are essentially sinusoidal in character, the order of magnitude of the inertial forces that arise because of the local fluid accelerations will be given by the product of the fluid density, ρ, the frequency of the oscillation, ω, the amplitude of the axial velocity fluctuation,

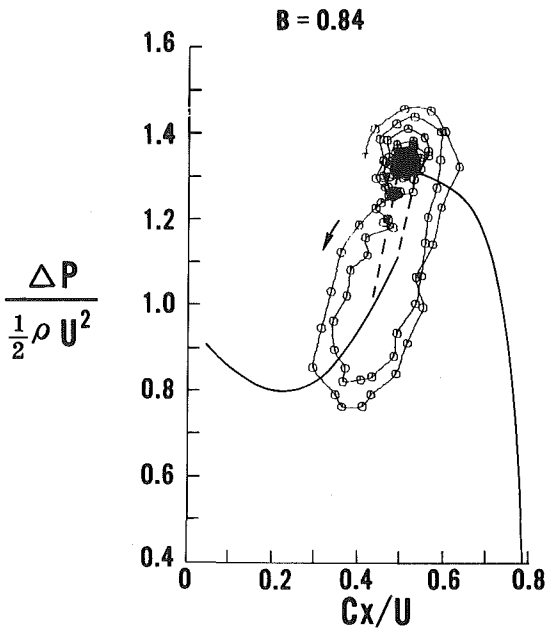

Fig. 10 Transient compression system response: $B = 0.84$

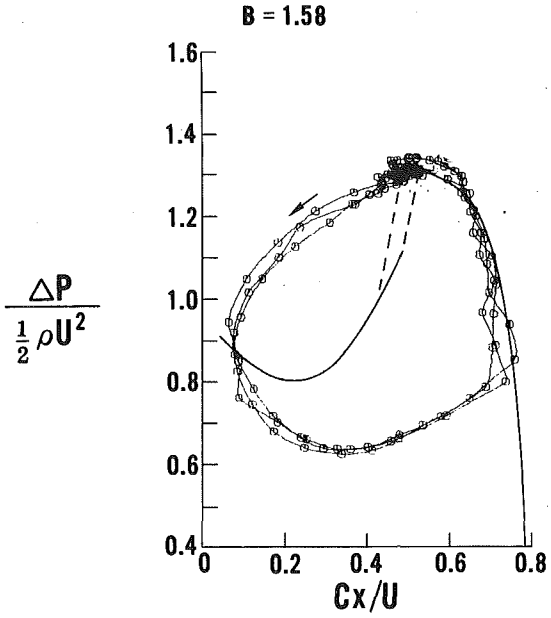

Fig. 12 Transient compression system response: $B = 1.58$

and the volume of the fluid in the duct, A_cL_c. Hence, if we assume for the moment that the axial velocity fluctuation is a specified fraction of the mean axial velocity, the order of magnitude of the inertial forces will be proportional to $\rho\omega UL_cA_c$. The ratio of the proportions of the two forces, pressure and inertial, is therefore given by B. Thus, as B is increased, for example by decreasing the duct length, a fixed percent amplitude of compressor axial velocity oscillations will result in inertial forces that are relatively smaller and smaller compared to the driving force due to the pressure differential. However, the magnitude of the driving pressure differential during the surge cycle is set primarily by the drop in the compressor pressure rise characteristic, and does not change substantially as B varies. Further, the oscillations shown in Figs. 8–12 are basically characterized by a balance between inertial and pressure forces so that the ratio of the two cannot actually decrease substantially but should remain fairly constant as B changes. There-

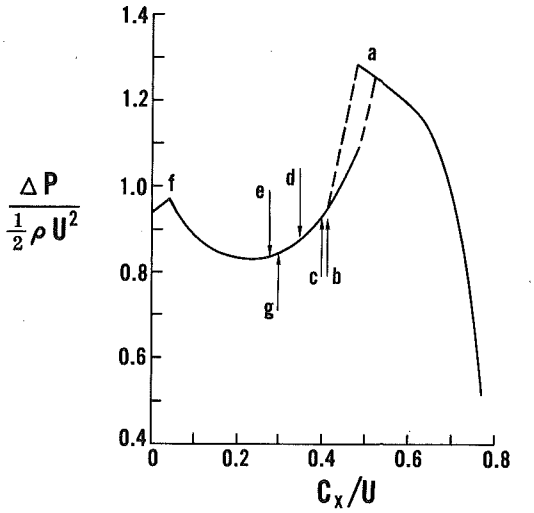

Fig. 13 Flow regime locations on compressor characteristic

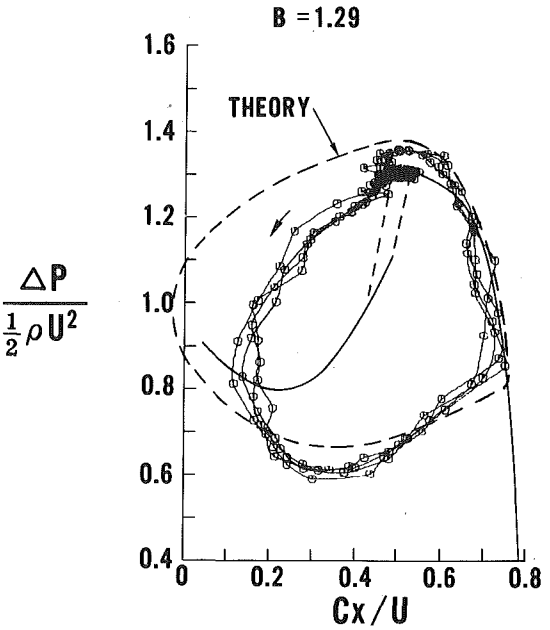

Fig. 11 Transient compression system response: $B = 1.29$

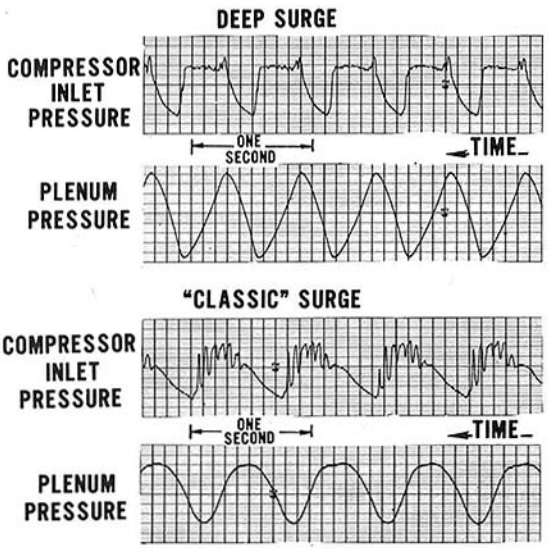

Fig. 14 Pressure oscillations during deep surge and classic surge

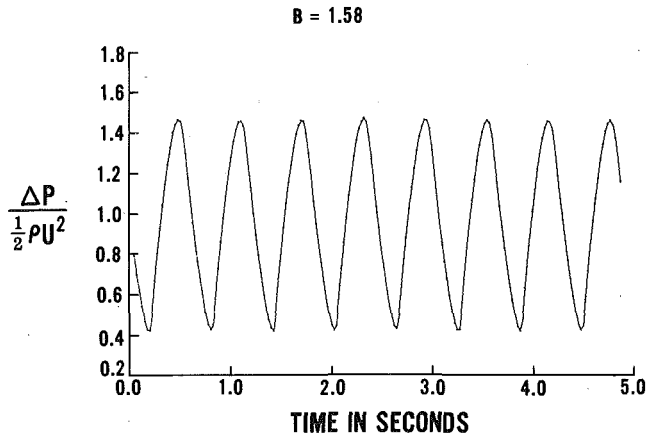

Fig. 15(a) Pressure oscillations during deep surge cycle: $B = 1.58$

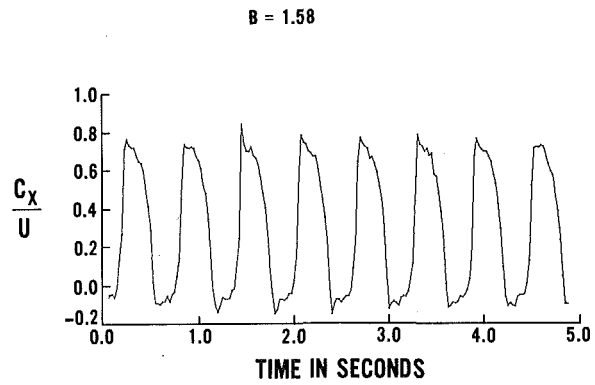

Fig. 15(b) Axial velocity oscillations during deep surge cycle: $B = 1.58$

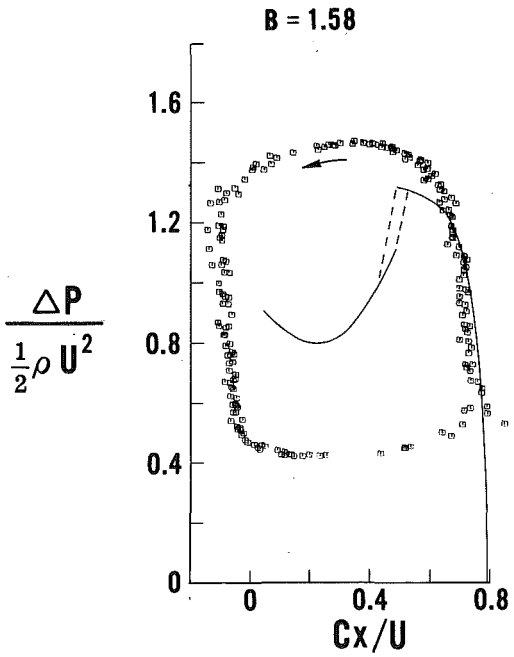

Fig. 15(c) Deep Surge Cycle: $B = 1.58$

fore, the relative amplitude of the axial velocity oscillations cannot remain constant, but must increase as B increases to maintain this balance, leading to the more circular limit cycle curves seen at the higher values of B.

This explanation is by no means an exact one, since the use of the quantity $1/\omega$ as a measure of the relevant time scale of the motion becomes less adequate as B becomes large and the oscillations lose their quasi-sinusoidal character. However data shows that this effect is not of primary importance over the limited range of B to which the arguments are applied here, and, hence will not materially affect their basic validity.

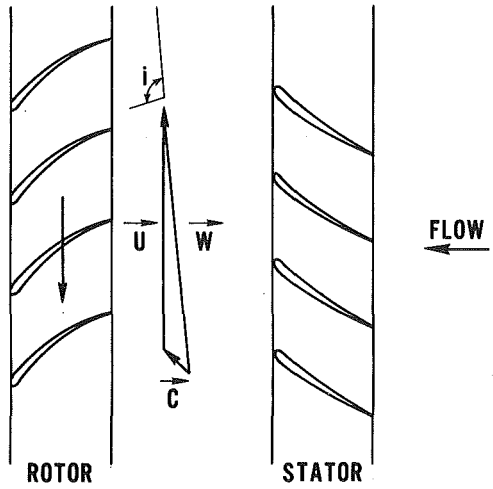

Fig. 16 Rotor mean velocity triangles during reverse flow

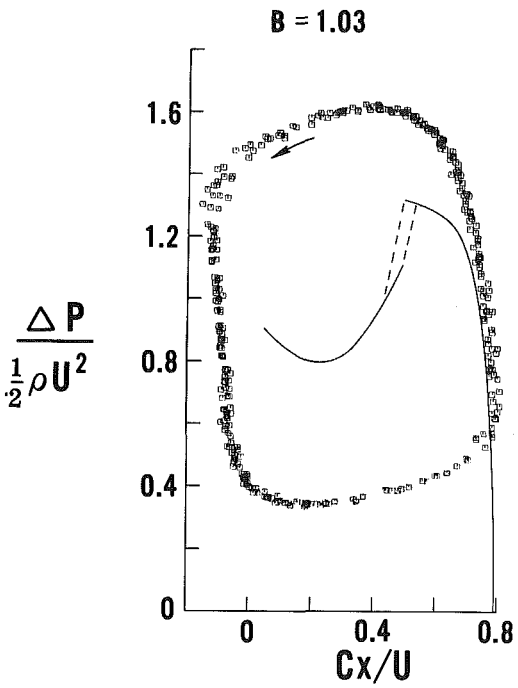

Fig. 17 Deep surge cycle: $B = 1.03$

"Classic Surge" and Deep Surge

In addition to the dependence on B, the unsteady behavior of the compression system can also be affected by changes in the steady-state equilibrium point of the system. In the present set of experiments this was determined by the downstream throttle area. Investigations were therefore carried out to determine how behavior would vary as the throttle area was changed at a constant compressor corrected speed. The changes were done in a basically quasi-steady fashion because of the nature of the throttle drive system.

It was found that two distinct sets of circumstances would occur, again depending on the value of B, with the dividing line between the two occurring at a value of B of approximately unity.

Let us consider the behavior at the higher values of B first, and describe what happens as the throttle area is decreased from some value that is associated with stable uniform flow operation. We can refer to Fig. 13, which shows the steady-state compressor characteristic. Initially the system is operating at point *a*. As the throttle area is decreased the compressor mass flow falls and a system instability results, leading at these values of B, to a surge cycle as shown in Figs. 8–12. For a throttle setting corresponding to a steady-state axial velocity parameter of 0.42 (point *b*), which is just beyond the stall limit, there are large amplitude oscillations in annulus averaged compressor flow and plenum pressure. During the cycle the compressor passes in and out of rotating stall as the instantaneous mass flow changes. If the throttle area is decreased slightly, corresponding to a decrease in C_x/U during steady-state operation to 0.40 (point *c*), the oscillations become more and more regular, and the frequency and amplitude change slightly. The oscillations at this point are still qualitatively the same as those in the preceding figures. However, a further decrease of the throttle area to a value that would correspond to a steady state C_x/U of approximately 0.35 (point *d*) leads to a marked change in the nature of the oscillations, with the amplitude and the frequency increasing significantly. The surge obtained at this and smaller throttle areas was qualitatively different from that previously described. It was labeled deep surge to distinguish it from the more classical type that was encountered with the higher flow rates at larger throttle areas. The difference between the two modes can be seen in Fig. 14 which shows static pressure versus time at the compressor inlet and in the plenum. All the traces, which are for the same value of corrected speed and plenum volume (i.e., the same B), but different throttle settings, have the same scale of vertical displacement to pressure difference. The differences in the frequency and amplitude of the oscillations can be clearly seen. In addition, although the compressor inlet static pressure traces show that rotating stall is occurring over a substantial part of the cycle in the classic surge oscillations, there is little evidence of rotating stall in the deep surges. The reason for this was not totally clear until the quantitative mass flow data was available. As will be seen below, from the results for the compressor axial velocity parameter as a function of time, it is apparent that there is a significant reverse flow during the deep surges. The decrease from a mass flow associated with (instantaneous) unstalled operation to a negative flow appears to be rapid enough to preclude the formation of a coherent stall cell pattern while the flow through the compressor is positive.

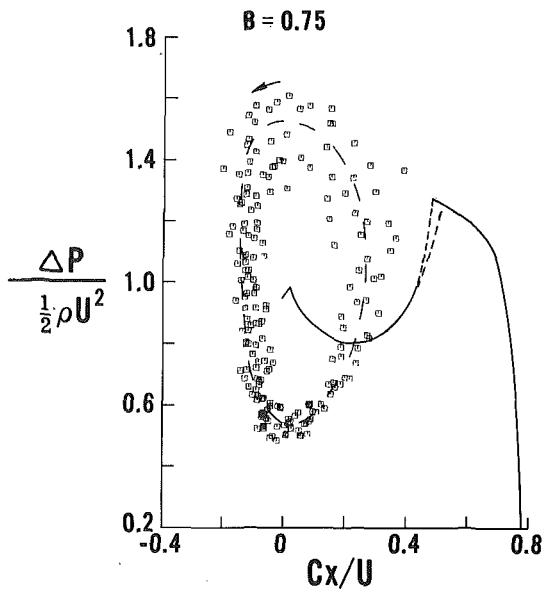

Fig. 18 Surge cycle at shut off throttle position: $B = 0.75$

The quantitative details of a deep surge oscillation that occurred with a throttle setting corresponding to point *e* are shown in Figs. 15*(a)*, 15*(b)*, and 15*(c)*, for a B of 1.58. In Fig. 15*(b)* it can be seen that the change of compressor mass flow with time is quite rapid over part of the cycle and quite slow over the rest. The shape of the axial velocity parameter/plenum pressure curve is also rather more squarish than those observed during classic surge. The sequence of events taking place during one of these oscillations can be described starting from the upper right-hand corner of one of these limit cycle paths as: (1) a rapid drop in compressor flow at roughly constant pressure to a negative flow, (2) a slow blowdown process where the compressor acts as a very high loss throttling device for the low velocity reverse flowing air, (3) a rapid change of mass flow at nearly constant pressure to a value associated with unstalled operation at large negative incidence on the compressor blades, and (4) a slow repressurization of the plenum during which the compressor mass flow changes quite gradually and the compressor operating point essentially moves along the steady state characteristic, finally reaching an axial velocity at which the blades stall, the compressor is no longer able to deliver the necessary pressure rise, and the cycle starts over again. The reason for the high pressure drop connected with the negative flow through the compressor can be understood if one draws compressor mean velocity triangles, as are presented for a rotor in Fig. 16. Because of the very small magnitude of the absolute velocity, the precise absolute angle of the flow incident on the rotor is not very important, and it can be seen that there can be an angle of incidence on the sharp *trailing edge* of the blades of more than 100 deg. Under such conditions one would expect the blading to be extremely effective in generating losses.

The deep surge oscillation persisted with little change in shape down to the lowest throttle setting that could be used, consistent with the limiting temperatures existing at very low flow rates. It was also found that there were throttle settings at which the two types of surge would appear intermittently.

The shape of the deep surge cycles was also influenced by the value of B. For comparison, Fig. 17 shows the deep surge encountered with the same compressor corrected speed and throttle setting, but with the 15.0 m^3 volume so that the value of B is 1.03. The same sequence of events is true here. Approximately 15 full cycles are shown in Fig. 17, and the oscillation can be seen to be extremely repeatable.

Surge/Rotating Stall Hysteresis at Constant Speed

At values of B lower than 1.0, a quite different pattern was found. As the throttle was closed from the initial setting for uniform flow operation, point a in Fig. 13, one obtained either classic

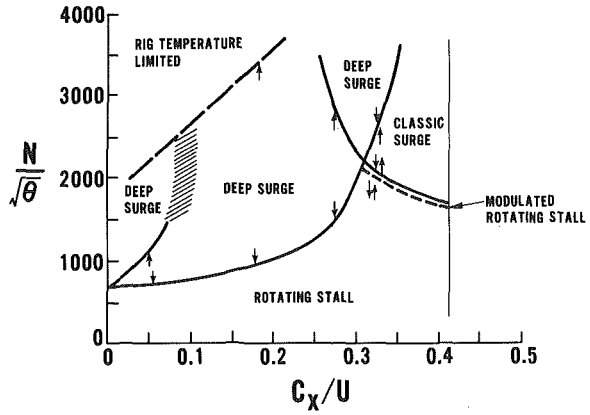

Fig. 19 Surge/rotating stall hysteresis along constant throttle lines: $V_p = 34.9$ m^3

surge or rotating stall at the stall limit line, depending on whether B was greater or less than 0.8 (see Fig. 6). However, even in the cases in which the system exhibited surge, when the throttle was closed further, to point *e*, say, the surging would cease and the compressor would operate in a stable rotating stall mode. According to the model developed in Part I, this was the expected behavior, since the calculations indicated that as the compressor was throttled away from the surge line, i.e., from point *b* to *c* to *d*. . . ., operation at the point defined by the intersection of throttle and compressor characteristics tended more towards stability. The reason for this is that the slope of the steady-state compressor curve becomes less and less positive as the flow is reduced, finally even becoming negative at a C_x/U of 0.2.

However, as the throttle area was decreased so that the axial velocity parameter was reduced to approximately 0.04 (point *f* in fig. 13), surge was again encountered.

Note that this point is associated with a compressor curve that has once again started to become positive. According to the analysis of Part I conditions would therefore appear to be more favorable for a surge cycle to develop, although a quantitative calculation cannot be done because of the lack of information about the precise nature of the compressor performance in the negative flow region.

The surge cycles at these low flow rates were similar to the deep surge previously described, as there is a negative flow through the compressor during a substantial part of the cycle. There was, however, one difference in that during the former the compressor operated in an unstalled condition over part of the cycle. During the deep surges encountered at the very low flow rates below point *f*, the axial velocities were not large enough for the compressor to become unstalled, and the inlet hot wires showed that unstalled operation was not achieved. These deep surges at low flow rates could be obtained at quite low values of B, and in fact, it was possible to detect them down to values of B as low as 0.4. The time dependent behavior during one of these surges at a "shut off" throttle setting is shown in Fig. 18 for a compressor speed of 44.0 m/s and a plenum volume of 34.9 m^3, corresponding to a B of 0.75. Because of the low value of pressure rise the estimated accuracy in the mass flow for this case is approximately ±8 percent, but it is apparent that the axial velocity parameter does not reach the value of approximately 0.5 that it must have for unstalled operation.

One of the interesting features of this type of surge was the large amount of hysteresis associated with it. The flow rate had to be decreased to point *f* for the initiation of surge. However, once started, surging would persist as the throttle was opened until approximately point *g* was reached, where steady rotating stall would again appear. This large amount of hysteresis that exists again emphasizes the strongly nonlinear behavior of the system, since the conditions at a point are not enough to predict the dynamic behavior, but rather the conditions over a finite region are necessary.

Surge/Rotating Stall Hysteresis at Constant Throttle

The large amount of hysteresis that existed in the rotating stall/surge boundary when operating at a constant corrected speed suggested that one could encounter this sort of behavior along constant throttle lines also. Therefore, some limited data were taken on the behavior of the system as one increased or decreased the rotor speed while holding the throttle constant. It was found that, similar to the behavior along a constant speed line, there was little or no hysteresis in the classic surge/rotating stall and classic surge/deep surge boundaries as the speed was changed. However, again, as found with the constant speed runs, there was a large amount of hysteresis in the onset and cessation of deep surge (i.e., at the deep surge/rotating stall boundary). A plot of the results is shown in Fig. 19. The horizontal axis is the axial velocity parameter and the vertical axis is the rotor corrected speed in RPM. The boundaries of the various regimes are indicated, with the arrows showing whether they refer to an approach direction of increasing or decreasing speed. Although only one region of modulated rotating stall is indicated in the figure, all of the boundaries do have some small zone surrounding them where the behavior undergoes a transition from one mode to the other. It should be noted that the limited data from the other volumes scales to this data as the square root of the plenum volume—in other words that a plot of C_x/U versus B correlates the different flow regimes very well.

Some explanation should be given of the manner in which the data was obtained. The throttle was first set at a low enough speed so that the compression system was operating stably in rotating stall. The speed was then increased to the maximum, the flow regimes that occurred being noted. The speed was then decreased. For some of the throttle settings it was possible to stay in rotating stall to the maximum speed. However at this speed the throttle settings could be changed to obtain surge and it was then possible to go back to the original throttle setting (still operating in surge) and start decreasing the speed down to a substantially lower value where the surge would stop. Again, therefore, one can see that the occurrence of the deep surge is associated with a meta-stable type of behavior in which a perturbation of a certain minimum size is required for the onset of sustained oscillations. The behavior of the compression system is thus not determined uniquely by (the intersection of) the throttle and the compressor characteristic curves and the relevant nondimensional parameter, B, but is dependent on the history of the path motion as well.

A Heuristic Model for Deep Surge

The deep surge model cannot be quantitatively predicted using the present model, since a knowledge of the nonsteady compressor performance in the low and negative flow region is critical. However, in order to attempt to understand the nature of this type of compression system oscillation, some exploratory parametric studies were carried out using the theoretical model. These were based on the following ideas: The rate of change of compressor mass flow, i.e., the acceleration of the fluid in the compressor duct, is quite small during the blowdown part of one of these cycles (see Fig. 15*(b)*). The pressure difference across the duct must therefore be approximately equal to the steady-state compressor pressure rise (as it is for example during the slow pressurization part of the cycle). The steeply negatively sloped part of the surge cycle in Fig. 15*(c)* or 17 that occurs at negative flows can therefore be used to represent the steady-state characteristic in this region. The most noticeable aspect of doing this is that the minimum pressure rises that are found during negative flow are substantially less than those that are measured during steady-state operations at zero flow. Hence, between essentially zero flow and some small negative value there should be a region where the compressor pressure rise curve has a strongly positive slope.

Calculations were therefore carried out using a compressor characteristic that consisted of the measured steady-state curve down to zero flow, the measured plenum pressure/axial velocity parameter curve from a deep surge for the negative flow part of the characteristic, and a (steeply positive) straight line joining the ends of the two measured curves. In terms of Fig. 17, for example, this third segment would be a straight line from the lower left hand "corner" of the cycle to the end of the steady-state curve. Due to the lack of information about the nonsteady compressor performance at negative flows, the calculations were done using a quasi-steady compressor response.

Over a range of values of B, it was found that if a large initial perturbation was imposed, the system would surge at a throttle setting such that the (unstable) equilibrium point was near the stall limit line (like point *c*, in Fig. 13, say) but would go into rotating stall if the throttle was closed so that the equilibrium point moved to a lower value of C_x/U. Further decrease of the throttle would again bring surge. The two calculated surge modes exhibited the basic differences seen experimentally: the surge observed at the lower flow rate showing a long blowdown time, a mass flow that did not become large enough to unstall the compressor at very low throttle settings, etc., while the other surge mode showed the characteristics of classic surge. There was also a strong effect of initial

conditions on the first type, in that if the initial perturbations were not large enough to make the compressor reach the negative flow region, a stable operation in rotating stall would result. This behavior is indicative of the hysteresis or path dependence seen with deep surge since if one approaches a given compressor/throttle intersection with the system surging it is equivalent to imposing a large initial perturbation, but if the system is in rotating stall and one approaches the same setting it is equivalent to having only a small initial perturbation, as the flow and pressure rise are basically steady.

As the value of B was increased the region of calculated stability (rotating stall) disappeared, the behavior going directly from one mode to the other as the throttle setting was changed, again in qualitative agreement with the data at the higher values of B.

The calculations were repeated with several different combinations of curves, and similar results were obtained over a range of reverse flow compressor characteristics. Thus, although, as stated, the calculations were carried out as an exploratory investigation, it would appear that the system exhibits many of the features of the deep surge mode. Hence, the occurrence of this type of surge may well be dependent on the existence of a sharp change in the compressor pressure rise as the mass flow is reduced past zero.

Influence of Compressor Effective Length

We have explored so far the effect of changes in rotor speed and plenum volume. The experiment was designed so that a further parameter, the effective length of the compressor duct, could be altered as well. This was done by adding 0.76 m of constant area annulus duct onto the compressor exit ducting to increase the effective length by approximately 45 percent.

It was found, however, that the addition of the extra ducting had an effect that prohibited a direct comparison of runs with and without the extension. This was that the compressor characteristic itself was altered. This is perhaps not unexpected when one remembers that the characteristic that is used is the overall one of plenum pressure minus atmospheric. With unstalled flow the characteristics with and without the extension were very closely similar, as the duct losses are small compared to the overall pressure rise and the duct exit conditions are not significantly different. When rotating stall is present, however, the situation is quite different. There are strong circumferential static pressure gradients in the duct downstream of the compressor. For example, measurements taken 0.31 m downstream of the compressor exit plane during rotating stall show that the static pressure variations are still more than three-quarters as large as they were at the compressor exit. (The compressor mean circumference is 1.61 m.) These large circumferential static pressure nonuniformities mean that significant streamline curvatures are occurring. Hence, since in one case there is a much longer axial length for accommodation to these gradients, it is to be expected that the velocity distribution at the duct exit would not be similar in the two cases.

As a result of the influence of the dissimilar flow fields on the compressor characteristic we cannot compare the extended duct results in a quantitative manner with the previous data. However, some pertinent comments can be made. First note that as predicted, the effect of the extension was to increase the rotor speed at which the compressor surged (for a given volume), although the increase was approximately ten percent higher than that calculated from the B = constant considerations. However, when the calculations for the critical value of B were redone using the compressor characteristic associated with the duct extension, it was found that the critical value of B needed for surge was also raised, in a similar fashion. Based on this result, it would therefore seem that the influence of length, when it can be separated from interacting with the compressor characteristic, is also correctly taken into account.

General Discussion of the Comparison Between Theory and Experiment

Two separate theoretical ideas about the transient behavior of an axial compression system have been developed in Part I and applied to the experimental results reported in this paper. The most basic is that the value of the nondimensional parameter B is the dominant factor governing the dynamic response of the system. This has been found to be a valid criterion for determining which mode of instability, rotating stall or surge, will occur at the stall limit line, as well as for the transient motion of the operating point. In addition, it appears that the dividing lines between the various stall flow regimes will also correlate very well with B when comparing data from different speeds or volumes.

The second concept is that the model that was developed in Part I is able to predict the detailed dynamic behavior of a compression system subsequent to the onset of instability of uniform flow. This has also been found to be basically valid for the stall line transients. The small discrepancy between the theoretical predictions and the data is thought to be mainly due to the simplified description of the unsteady response of the compressor, since the actual instantaneous pressure rise delivered by the compressor is still not well documented. However, the approximation used in the model appears to be adequate in these situations.

In contrast, one can obtain only qualitative trends concerning the deep surge and low flow rate deep surge, where a substantial part of the cycle is spent with negative flow through the compressor. The reason for this is felt to be the fundamental lack of knowledge about the unsteady compressor performance in the low or negative mass flow regimes, which is needed in order to model the overall system behavior in a more quantitative fashion.

Summary and Conclusions

1 An experimental investigation of axial compressor surge and rotating stall has been conducted using a three stage axial flow compressor.

2 The theoretical compression system model that was developed in Part I has been found to give adequate predictions of compressor response for the rotating stall and surge transients at the stall limit line.

3 As predicted, the dynamic response of the system is found to depend strongly on the value of the nondimensional parameter, B, which can be defined in terms of the resonant frequency of the system as $B = U/(2\omega L_c)$; or, equivalently, in terms of the physical system parameters as $B = (U/2a)(V_p/A_cL_c)^{1/2}$. In particular, if speed and plenum volume are varied independently, the boundary between rotating stall and surge occurs at a constant B. Further, the motion of the compressor operating point will also be the same if B is maintained constant, whatever the values of the individual dimensional system parameters.

4 A data analysis procedure has been developed which is able to provide the first quantitative information about the instantaneous system operating point (i.e., pressure rise and annulus averaged compressor mass flow) during surge and rotating stall transients.

5 Two distinct types of compressor surge cycles have been identified. The first is called classic surge. In this mode, the compressor can be seen to pass in and out of rotating stall as the mass flow changes during the cycle. In the second type, called deep surge, a significant part of the cycle is spent with the compressor operating at a negative flow. No coherent rotating stall pattern is seen.

6 Depending on the value of B, as the exit throttle area was decreased, the compression system exhibited three types of behavior. At values of B larger than approximately 1.0, first classical surge and then deep surge was encountered. At values lower than this, but above 0.8, the sequence was classic surge, rotating stall, then deep surge. Finally, at values of B lower than 0.8, the system exhibited just rotating stall, and then deep surge.

7 The deep surge mode has a large amount of hysteresis associated with its onset and cessation. Therefore, the dynamic compressor behavior is not uniquely determined by the speed and the throttle setting, but the time history of the setting of the operating point must be specified. The quantitative modelling of this type of

surge will require further investigation of the unsteady response of an axial compressor to a rapid change in mass flow.

Acknowledgment

The author wishes to thank Pratt & Whitney Aircraft, Division of United Aircraft Corporation, East Hartford, Connecticut, for permission to publish this paper. The author is also indebted to Mr. M. B. Christianson for his efforts in support of the test program and to Mr. H. A. Droitcour for his invaluable contributions to the development of the data analysis procedure.

APPENDIX

Justification of the Data Analysis Procedure

The purpose of the following discussion is to demonstrate that an isentropic representation of the process occurring in the plenum gives sufficient accuracy in the calculation of $\dot{m}_1$.

As developed in the body of the paper, the continuity equation and the First Law for the plenum (equations (7) and (10)) can be written:

$$\dot{m}_1 = \dot{m}_2 + V_p \frac{d\rho_p}{dt} \tag{A-1}$$

$$\dot{m}_1 \frac{T_{0_1}}{T_p} = \dot{m}_2 + \frac{\rho_p V_p}{\gamma P_p} \frac{dP_p}{dt} \tag{A-2}$$

The nomenclature is the same as that defined by Fig. 4.

If an isentropic relationship is assumed for the plenum, the continuity equation becomes

$$\dot{m}_{1_{\text{isen}}} = \dot{m}_2 + \frac{\rho_p V_p}{\gamma P_p} \frac{dP_p}{dt} \tag{A-3}$$

The mass flow $\dot{m}_{1\text{isen}}$ is the compressor exit mass flow that would be calculated using the isentropic relation. The effect of calculating $\dot{m}_1$ in this manner is thus to introduce an error, ϵ, which is defined by

$$\epsilon = \dot{m}_1 - \dot{m}_{1_{\text{isen}}} \tag{A-4}$$

Therefore,

$$\epsilon = (1 - \frac{T_{0_1}}{T_p})\dot{m}_1 \tag{A-5}$$

We can now use typical data to estimate the largest magnitude of this error that might be encountered. This will occur at the highest speed that was run since the temperature differences scale as U^2. Let us write:

$$T_{0_1}(t) = \bar{T}_{0_1}[1 + \delta T_{0_1}(t)/\bar{T}_{0_1}] \tag{A-6}$$

$$T_p(t) = \bar{T}_p[1 + \delta T_p(t)/\bar{T}_p] \tag{A-7}$$

To estimate the fluctuation in T_p, we assume a polytropic process in the plenum with polytropic exponent k. Thus:

$$T_p \cong \bar{T}_p[1 + \frac{k-1}{k} \cdot \frac{\delta P_p}{\bar{P}_p}] \tag{A-8}$$

The data shows that the magnitude of the term $\delta P_p/\bar{P}_p$ is,

$$\frac{\delta P_p}{P_p} \leq 0.03 \tag{A-9}$$

Hence, substituting in the numbers for T_p, we find that δT_p is on the order of 3 °K or less for polytropic exponents from 1.0 to 1.6, a range that represents far larger departures from isentropy than are obtained in the processes under consideration. A conservative maximum estimate for δT_p is thus 3 °K. This would occur during the more violent deep surges, with the magnitude during any of the classic type of surges being only two degrees.

To estimate δT_{0_1}, we can use data and assume that the compressor behavior is quasi-steady. Again this will tend to lead us to an overestimate so that our answer will indicate an upper bound. Let us calculate δT_{0_1} for two flow rates—a very low, but positive, one and a high one—such as might be associated with the minimum and maximum flow rates encountered during a classic surge type of oscillation. Data gives:

$$@\dot{m}_{1_{\min}};\ \delta T_{0_1}/\bar{T}_{0_1} < 0.04 \tag{A-10}$$

$$@\dot{m}_{1_{\max}};\ \delta T_{0_1}/\bar{T}_{0_1} < 0.01 \tag{A-11}$$

Since the plenum is adiabatic, we can take

$$\bar{T}_{0_1} \cong \bar{T}_p \tag{A-12}$$

Then

$$\epsilon/\dot{m}_1 = (1 - T_{0_1}/T_p) \cong \frac{(\delta T_p - \delta T_{0_1})}{\bar{T}_p} \tag{A-13}$$

Again substituting numbers and taking account of the phasing of δT_p and δT_{0_1}, we can arrive at an estimate of the maximum relative error in $\dot{m}_1$. At the two flow rates:

$$@\dot{m}_{1_{\min}};\ \epsilon/\dot{m}_1 \simeq 0.04 \tag{A-14}$$

$$@\dot{m}_{1_{\max}};\ \epsilon/\dot{m}_1 \simeq 0.015 \tag{A-15}$$

However, what we are really concerned about is the absolute error in $\dot{m}_1$, or the error relative to the mean value of $\dot{m}_1$, for example, the time averaged value, $\bar{\dot{m}}_1$.

$$\epsilon/\bar{\dot{m}}_1 = \frac{\dot{m}_1}{\bar{\dot{m}}_1}(1 - T_{0_1}/T_p) \tag{A-16}$$

At $\dot{m}_{1_{min}}$ and $\dot{m}_{1_{max}}$ we have:

$$\frac{\dot{m}_{1_{\min}}}{\bar{\dot{m}}} \simeq 0.1 \tag{A-17}$$

$$\frac{\dot{m}_{1_{\max}}}{\bar{\dot{m}}} \simeq 2 \tag{A-18}$$

Therefore,

$$\epsilon/\dot{m}_1 \simeq 0.03 \text{ at } \dot{m}_{1_{\max}} \tag{A-19}$$

$$\epsilon/\bar{\dot{m}}_1 \simeq 0.004 \text{ at } \dot{m}_{1_{\min}} \tag{A-20}$$

The use of the data to make the calculation at other values of $\dot{m}_1$ shows that:

$$\epsilon/\bar{\dot{m}}_1 < 0.03, \tag{A-21}$$

due to the isentropic assumption, which is comparable to or less than the experimental error involved in calculating $\dot{m}_1$. Since this is an estimate of the maximum error, and the actual error will in general be less than this, the isentropic assumption is justified for the approximate calculation procedure.

Finally it can be noted that there are situations, such as the deep surge cycles, where the flow is negative over a considerable part of the cycle. When this occurs the two sources of entropy changes in the plenum—namely the inflow of fluid with a different entropy than the fluid already in the plenum, and the mixing of the incoming fluid with that already in the plenum—are absent. Thus, during negative flow (outflow from the plenum through the compressor), the isentropic assumption should be even more accurate than the foregoing estimate.